Final Report for AOARD Grant FA2386-12-1-4042

"Biomaterial-based Memory Device Development by Conducting Metallic DNA"

Date: May 28, 2013

Name of Principal Investigators (PI and Co-PIs): Chia-Ching Chang
- e-mail address : ccchang01@facu;ty.nctu.edu.tw
- Institution : NATIONAL CHIAO TUNG UNIVERSITY
- Mailing Address : 1001 TA HSUEH RD HSINCHU 30056, TAIWAN
- Phone : +886-3-5731633
- Fax : +886-3-5733259

Period of Performance: May/02/2012 – May/01/2013

Abstract:

In this grant year a simple two terminal conducting DNA device was developed. This device exhibit the negative differential resistance (NDR) effect at room temperature. Moreover, we found the conductivity of this device could be affected by the history of the bias applied previously. By systematically studies, we found that both conducting and memory effect can be attribute to the redox reaction of Ni ions in the DNA nano-wire. Moreover, the redox state of Ni ions in DNA can change the resistance of Ni-DNA by applying different polar bias and time. Therefore, we have created a multiple-states memory system. This is the first multi-states resistance memory device by using bio-nanowire of the world. Based on this achievement, logic device and application will be developed in the near future, too. Moreover, by using Ni-DNA detection system, the protein-DNA interaction can be detected.

Introduction:

DNA is one of the most promising one-dimensional nanomaterials because of its adjustable length and self-assembly properties[1-4]. Although, the electron transfer properties of DNA were studied intensively for decades. Either conductor[3], semiconductor[5] or insulator[6] of DNA had been postulated. Therefore, the conclusions on DNA conductivity remained contradictory. Since intrinsic DNA conductivity cannot provide a convincing conclusion, by doping Ni ions into DNA, the conductivity of DNA increases significantly[4, 7]. On the basis of the redshift of UV absorption spectra, we think that the incorporation of metal ions may result in a reduction of the original DNA band gap and also an increase in the overlap between the states of the bases[4, 8]. These results indicate that the incorporation of nickel ions converts double-stranded DNA into a conducting wire through the improvement in charge transport via the stacking corridor[9]. This also indicated that the Ni-DNA acted like a coaxial cable. Namely the electron transport via the Ni-ions mediates stacking corridor and the backbone provide the conducting barrier to avoid intermolecular electron leakage[10]. Moreover, a molecular device that is fabricated from metallic deoxyribonucleic acid (M-DNA) exhibits a negative differential resistance (NDR) behavior at room temperature[11].

It is known that a memory resistors (memristor) is a type of passive circuit elements and its resistance varies according to a "history" of applied voltage or currents on a device[12]. The material implementation of memristive effects can be determined in part by the presence of hysteresis such as negative differential resistance (NDR) effect[13]. The first memristor was fabricated by the team of HP Lab in 2008[13]. This article was the first to demonstrate that a solid-state device could have the characteristics of a memristor based on the changing of the boundary between the high-resistance and low-resistance layers of titanium dioxide TiO_2 and TiO_{2-x}[13]. Their memristors require less energy to operate and they can store at least twice as much data in the same area[13]. Additionally, memristors can be used in digital logic as programmable switches in switching blocks[14]. Since Ni-DNA possess both NDR effect and its resistance correlates to a "history" of applied voltage or currents. Therefore, the Ni-DNA device can be developed as a memristors.

To fabricate the Ni-DNA based memristor, linear DNA (~2 kb) were obtained from Rop-tat plasmid[15], and they were metallized with Ni ions by our preexisting approaches[10-11]. The Ni-DNA was linked on two gold electrodes through the gold-thiol linkage. The gold electrodes were fabricated by using a standard e-beam lithography procedure. Their electrical properties were measured in ambient

Report Documentation Page

Form Approved
OMB No. 0704-0188

1. REPORT DATE	2. REPORT TYPE	3. DATES COVERED
30 MAY 2013	**Final**	**02-05-2012 to 01-05-2013**

4. TITLE AND SUBTITLE
Biomaterial-based Memory Device Development by Conducting Metallic DNA

5a. CONTRACT NUMBER
FA23861214042

5b. GRANT NUMBER

5c. PROGRAM ELEMENT NUMBER

6. AUTHOR(S)
Chia-Ching Chang

5d. PROJECT NUMBER

5e. TASK NUMBER

5f. WORK UNIT NUMBER

7. PERFORMING ORGANIZATION NAME(S) AND ADDRESS(ES)
National Chiao Tung University,R203, Bio-Lab II, Po-Ai Street,Hsinchu 300,Taiwan,TW,300

8. PERFORMING ORGANIZATION REPORT NUMBER
N/A

9. SPONSORING/MONITORING AGENCY NAME(S) AND ADDRESS(ES)
AOARD, UNIT 45002, APO, AP, 96338-5002

10. SPONSOR/MONITOR'S ACRONYM(S)
AOARD

11. SPONSOR/MONITOR'S REPORT NUMBER(S)
AOARD-124042

12. DISTRIBUTION/AVAILABILITY STATEMENT
Approved for public release; distribution unlimited

13. SUPPLEMENTARY NOTES

14. ABSTRACT

In this report a simple two terminal conducting DNA device was developed. This device exhibit the negative differential resistance (NDR) effect at room temperature. Moreover, we found the conductivity of this device could be affected by the history of the bias applied previously. By systematically studies, we found that both conducting and memory effect can be attribute to the redox reaction of Ni ions in the DNA nano-wire. Moreover, the redox state of Ni ions in DNA can change the resistance of Ni-DNA by applying different polar bias and time. Therefore, we have created a multiple-states memory system. This is the first multi-states resistance memory device by using bio-nanowire of the world. Based on this achievement, logic device and application will be developed in the near future, too. Moreover, by using Ni-DNA detection system, the protein-DNA interaction can be detected.

15. SUBJECT TERMS
BioNano Systems, Memristors, DNA Devices

16. SECURITY CLASSIFICATION OF:			17. LIMITATION OF ABSTRACT	18. NUMBER OF PAGES	19a. NAME OF RESPONSIBLE PERSON
a. REPORT	b. ABSTRACT	c. THIS PAGE			
unclassified	**unclassified**	**unclassified**	**Same as Report (SAR)**	**6**	

by a high-impedance electrometer. Two-probe measurements were imposed to take current-voltage (*I-V*) characteristics and memory device performances of the Ni-DNA memristor. In these measurements, current flowing through the Ni-DNA was obtained when the bias voltage was supplied on the two gold electrodes. Namely, we have created a voltage controlled resistance memory by Ni-DNA and this is a first green and bio-degradable molecular device.
For biosensing part, the interaction between p53 and Bax promoter sequence can be detected via the Ni-DNA electro-impedance spectroscopy.

Experiment:

1. **Ni-DNA synthesis**

All chemicals, unless otherwise noted, were purchased from Merck (Rahway, NJ) and Sigma (St. Louis, MO). The DNA linkers and the reagent used for staining DNA (Health View Nucleic Acid Stain) were purchased from Biokit (MiaoLi, Taiwan). Rop-tat plasmid[15] was kindly provided by Dr. Ru-Chih C. Huang as a gift. Rop vector was digested by BamHI and EcoRI to form linear DNA (~ 2 kb) with two sticky ends. Ni-DNA duplex with a final concentration of 1 μM was formed in a Ni^{2+} buffer (10 mM Tris, 2.5 mM NiCl2, pH = 9.0). The excess Ni^{2+} was removed by dialysis in the Tris buffer (10 mM Tris, pH = 9.0).

2. **Substrate and Ni-DNA nanowire device fabrication**

Silicon wafer with a layer of 300 nm- thick Silicon dioxide on top was employed as substrate to construct Ni-DNA nanowire device. The Ti/Au (~20/100 nm in thickness) electrodes were fabricated on the substrate by standard electron beam lithography and thermal evaporation. After electrodes fabrication, field emission scanning electron microscope (FESEM, JEOL JSM-6500F) was used to measure the morphology of patterned substrate. The gap width and length between electrodes are both approximately 100 nm. The insulation of background was determined by a high-impedance electrometer (Keithley 6517b, company name city and Country). The resistances between bare electrodes were over 10^{12} Ω. The cohesive ends Ni-DNA molecules were linked with gold electrodes through the thiol modified BamHI and EcoRI linkers those formed SAM structure on the gold electrodes.

3. Electrical properties measurement

All the electrical properties were carried out in ambient by the same electrometer mentioned above. Two-probe measurement configuration was used to measure *I-V* characteristics and characterize the behavior of memory device. Voltage bias was applied across the fabricated electrodes and the current flow through the Ni-DNA nanowires was measured.

4. Electro-impedance spectroscopy (EIS) analysis of p53-DNA interaction

All electrochemical measurements were performed with a 3-electrode cell. These electrodes included a modified Au electrode (working electrode), a coiled platinum wire (counter electrode), and an Ag/AgCl wire immersed in 3 M KCl (reference electrode). All experiments were performed at room temperature, and all potentials in this work were measured with direct relevance to the Ag/AgCl reference electrode. The EIS operates with a 10 mV AC sinusoidal amplitude and a 0.23 V (vs Ag/AgCl) direct current (DC) potential, which is the standard oxidizing potential of 2.5 mM $Fe(CN)_6^{4-/3-}$ (1:1 in 10 mM PBS solution [pH 7.4]), and a frequency ranging from 1 Hz to 10^5 Hz. $Fe(CN)_6^{4-/3-}$ acted as a redox substance in this study. ZSimpWin V3.20 software from Informer Technologies Inc. (Tennessee, USA) was used for simulation to reveal the related electrical parameters of the working electrode. The working electrode is modified with Bax ni-DNA. Each diluted p53 was detected repeatedly 3 times with different working probe. The parameters of Nyquist plot was calculated by Zsimp Win 3.2 and was showed as mean ± standard deviation (SD).

Results and Discussion:

In the Figure 1 the fluorescence of DNA which were stained with DNA dye could not be observed in Ni-DNA (lane 2) and could be observed at native DNA (lane 1) as well as 100 mM EDTA treated Ni-DNA (lane 3). Those results indicated that the Ni ions are correctly binding to duplex DNA at pHs above 8 and the metal chelating process is reversible.

1. Capacitive-Memristor of Ni-DNA

Figure 2 shows a cyclic sweep of the dynamic *I-V* characteristic of the Ni-DNA device at room temperature in ambient conditions. The *I-V* curves show obviously a hysteretic loop and a feature of NDR that indicate the emergence of a memristive like system[12]. The current reaches the maximum at a voltage of $E_{p,a}$ near 5 V that points to the oxidation process. The current decreases at higher voltages. It is reduced further as the voltage sweeping back from +9 V to 0 V. The current is not zero when the

voltage sweeps back to zero which is unlike the initial condition of zero current at zero voltage (see the inset to Figure 2). The non-zero current could come from the parallel capacitance in Ni-DNA that will be addressed later. A further sweep to -9 V gives another current peak at a voltage of $E_{p,c}$ near -5 V that implies the reduction process from Ni^{3+} back to Ni^{2+} ions. It is noted that the cyclic redox reaction shown in the *I-V* sweeping has never been observed in native DNA devices (data not shown). It confirms in agreement with our previous report[11] again that the introduction of Ni ions initiates the high conductivity and the redox property in Ni-DNA.

2. Mechanism analysis.

As indicated previously the resistance of Ni-DNA may variate according to the history of applied voltage or current. Here, we propose a model of capacitive memristive system to illustrate the I-V characteristic of Ni-DNA. The definition of memristive system can be descibed by the equations[12]

$$V = R(w,i)i \quad (1)\,; \quad \frac{dw}{dt} = f(w,i) \quad (2)$$

where w is a set of state variables, and *R* and *f* are explicit functions of time.

When the current flows through the Ni-DNA device, redox occurs for Nickel ions embeded in the DNAs:

$$Ni^{2+} \underset{reduction}{\overset{oxidation}{\rightleftharpoons}} Ni^{3+} + e^{-},$$

where the number of Ni^{2+} (Ni^{3+}) ions varies due to the oxidation-reduction processes caused by the alternating current flowing between the left and right electrodes, as shown in Figure 3(a). The total resistance of the Ni-DNA device is proportional to the number of Ni^{2+} and Ni^{3+}, as shown in Figure 3(b), similar to the TiO_{2-x} memristive system proposed by HP Laboratory[13]. The oxidation-reduction processes create charge accumulation in the Ni-DNA region in the device due to emission and absorption of electrons. The charge acummuation generates another source of electric current proportional to the rate of change in the total number Ni^{3+} ions.

Compared with the large current at the order of mA in TiO_{2-x} memristive system, the current in the Ni-DNA device is of the order of nA due to the large total resistance. At the same time the charge may go through the DNA π–π stacking corridor. Consequently, the drift current drived by the alternating bias is strongly suppressed due to the larg e resistance such that the current owing to charge accumulated in the Ni-DNA region becomes important. The charge accumulation introduces an impedance due to capacitor effect and a current relevant to the redox. Such a capacitive memristor generates hitherto unreported current-voltage characteristic beyond the description of memristor. The most striking feature in this capacitive memristor system is the non-vanishing current at zero bias in the hysteresis I-V curve.

The current-voltage hysteresis loop, can be expressed as following:

$$I(t) = I_{drift}(t) + \tilde{I}(t) \quad (3)$$

I_{drift} (t) denoted the drift current, and $\tilde{I}(t)$ denoted the charge accumulation,

The drift current driven by the external alternating bias $V(t) = V_0 \exp(i\omega t)$,

$$I_{drift}(t) = Re\{\frac{V(t)}{Z}\}, \quad (4)$$

where the impedance Z includes the capacitive contribution,

$$\frac{1}{Z} = \frac{1}{R(t)} + \frac{1}{\frac{1}{i\omega C}}, \quad (5)$$

where C is the capacitance owing to charge cumulation and $R(t)$ is the total resistance described by the resistor model considered similar to the memristor model proposed by HP Lab.[13],

$$R(t) = [1 - N(t)/N_0]R_{2+} + [N(t)/N_0]R_{3+}, \quad (6)$$

where N_0 is the total number of Ni^{2+} and Ni^{3+} ions in the Ni-doped DNA device; *N(t)* is total number of Ni^{3+} ions; R_{2+} and R_{3+} denote the resistances when all *Ni* ions in the device are

completely in Ni^{2+} and Ni^{3+} states, respectively. Namely, the N(t) is a set of state variables (w) in equation 1 and 2. The charge dynamics is relevant to redox reaction. The rate of change in $N(t)$ is given by,

$$\frac{dN(t)}{dt} = k_{ox}(T)(N_0 - N(t)) - k_{red}(T)N(t), \qquad (7)$$

where $k_{ox}(T)$ and $k_{red}(T)$ represent the temperature-dependent oxidation and reductio rate constants, respectively. The rate constants are estimated by the Arrehenius rate equations,

To know the form of the current $\tilde{I}(t)$ in Eq. (1), we assume that the gradient of the chage density causes a diffusive current. The concentration of the Ni^{3+} ions at position x at a particular time t is denoted as $n(x,t)$ and a shematic of $n(x,t)$ is shown in Figure 3c. Owing to the charge accumulation, the current flows through the surface of the left electrode [$I(x=0,t)$] into the Ni-DNA region is different from that flows through the surface of the right electrode [$I(x=L,t)$] out of the Ni-DNA region. Considering the equation of continuity, the diffusive currents at the left and right surface of the electrodes satisfy the following equation,

$$I_{diff}(x=L,t) - I_{diff}(x=0,t) = e\frac{\partial}{\partial t}N(t), \qquad (8)$$

where $N(t) = \int_0^L n(x,t)dx$ is the total number of Ni^{3+} ions in the Ni-DNA device and $I_{diff}(x,t) = eD\frac{\partial}{\partial x}n(x,t)$ is the diffusive current at position x and time t. We assume that $I_{diff}(x=L,t)$ and $I_{diff}(x=0,t)$ are different but self-similar as a function of time such that $\tilde{I}(t) \equiv I_{diff}(x=0,t) = cI_{diff}(x=L,t)$, where c should be a constant which is close to 1. As a direct result of Eq. (10), the current $\tilde{I}(t)$ in Eq. (3) is,

$$\tilde{I}(t) = fe\frac{\partial}{\partial t}N(t), \qquad (9)$$

where $f = 1/(1-c)$ is a parameter to be fitted by the experimental data which is much larger than 1.

The simulation result was compared with experimental data in Figure 2. The agreement between simulation and experiment shows the validity of this physical model.

3. memory device

According to theoretical calculations and arguments based on cyclic *I*-*V* measurements, the two-terminal Ni-DNA device can be employed as a memory device. In addition and more intriguingly, the Ni-DNA memory device can be set to operate at multiple states with the state variable *N*(*t*). The state of the Ni-DNA memory deice can be set with an operating voltage larger than the redox potential and the multiple state writing can be achieved by controlling the writing time t_w. Alterntively, the state can be read out at a reading voltage much lower than the redox potential. The idea was realized as follows. The voltage supplied on the Ni-DNA memory device for writing and reading is portrayed in Figure 3a and its corresponding current is displayed in Figure 3b. The blue (red) line in Figure 4a presents a writing of oxidixed (reduced) state of Ni ions at +6 V (-6V). The writing time t_w is varied from 1 to 500 s in this experiment. The black lines in Figure 4a show the reading voltage of ±1 V which is intentionally imposed with a slow rising speed from 0 V and controlled by the dwelling time t_d. The reading voltage is kept the same for the remaining reading time. Before any writing operations, the current outputs of the Ni-DNA memory device follow the black lines shown in Figure 4b. At both positive and negative reading voltages, the read-out current exhibits a symmtric manner of time dependence and reaches a stable current at a longer time. From the microscopy scope, this behavior is owing to the different ratio of Ni^{3+} and Ni^{2+}. From our physical model, the resistance of Ni-DNA is described as $R(n(t_w,V))$, where *V* is the applied bias voltage. If one can control the ratio by varying the writing time and applied bias voltage precisely, 2N states can be achieved, where N is the number of Ni-ion imbedded which is corresponding to the number of the DNA base pairs[10]. This property

implied that Ni-DNA can be used as high density memory device.

4. Biosensing analysis of interactions between p53 and Bax promoter

The Ni-DNA of Bax SAM was performed on the gold electrode and the R_{ct} of Ni-DNA SAM was 32.05 KΩ. The R_{ct} increased to 81.59 KΩ when the p53 presented (Figure 4). This result indicates the sequence of Ni-DNA can be recognized by its target protein even with Ni ions chelation. Therefore, this detection method can be used widely in protein-DNA interaction, especially for promoter assay.

In summary, we have synthesis the Ni-DNA synthesis and device fabrication. A green memory device has developed and its memory effect has been characterized. Moreover, this Ni-DNA technique can be used for biosensing. Namely, we have achieved all aims of our project.

List of Publications and Significant Collaborations that resulted from your AOARD supported project:

The manuscript is in preparation and will be submitted soon.

DD882: As a separate document, please complete and sign the inventions disclosure form.

References:

(1) Aviram, A.; Ratner, M. A. *Chemical Physics Letters* **1974,** *29,* 277-283.
(2) Mirkin, C. A.; Letsinger, R. L.; Mucic, R. C.; Storhoff, J. J. *Nature* **1996,** *382,* 607-609.
(3) Hwang, J. S.; Hwang, S. W.; Ahn, D. *Superlattices and Microstructures* **2003,** *34,* 433-438.
(4) Peng-Chung Jang, J.; Tzeng-Feng, L.; Chuan-Mei, T.; Ming-Shih, T.; Chia-Ching, C. *Nanotechnology* **2008,** *19,* 355703.
(5) Porath, D.; Bezryadin, A.; de Vries, S.; Dekker, C. *Nature* **2000,** *403,* 635-638.
(6) de Pablo, P. J.; Moreno-Herrero, F.; Colchero, J.; Gómez, H., J.; Herrero, P.; Baró, A. M.; Ordejón, P.; Soler, J. M.; Artacho, E. *Physical Review Letters* **2000,** *85,* 4992-4995.
(7) Rakitin, A.; Aich, P.; Papadopoulos, C.; Kobzar, Y.; Vedeneev, A. S.; Lee, J. S.; Xu, J. M. *Physical Review Letters* **2001,** *86,* 3670-3673.
(8) Alexandre, S. S.; Soler, J. M.; Seijo, L.; Zamora, F. *Physical Review B* **2006,** *73,* 205112.
(9) Liu, T.; Barton, J. K. *Journal of the American Chemical Society* **2005,** *127,* 10160-10161.
(10) Tseng, S.-H.; JangJian, P.-C.; Tsai, C.-M.; Cheng, T.-M.; Chu, H.-L.; Chang, Y.-C.; Chung, W.-H.; Chang, C.-C. *Biophysical Journal* **2011,** *100,* 1042-1048.
(11) Jangjian, P.-C.; Liu, T.-F.; Li, M.-Y.; Tsai, M.-S.; Chang, C.-C. *Applied Physics Letters* **2009,** *94,* 043105-3.
(12) Di Ventra, M.; Pershin, Y. V.; Chua, L. O. *Proceedings of the IEEE* **2009,** *97,* 1717-1724.
(13) Strukov, D. B.; Snider, G. S.; Stewart, D. R.; Williams, R. S. *Nature* **2008,** *453,* 80-83.
(14) Xia, Q.; Robinett, W.; Cumbie, M. W.; Banerjee, N.; Cardinali, T. J.; Yang, J. J.; Wu, W.; Li, X.; Tong, W. M.; Strukov, D. B.; Snider, G. S.; Medeiros-Ribeiro, G.; Williams, R. S. *Nano Letters* **2009,** *9,* 3640-3645.
(15) Giza, P. E.; Huang, R. C. C. *Gene* **1989,** *78,* 73-84.

Figure legends:

Figure 1.The fluorescence image of DNAs. M, 1, 2, and 3 denote DNA marker, native DNA, Ni-DNA, and Ni-DNA treated with 100 mM EDTA, respectively.

Figure 2. Scan rate dependent *I-V* characteristics of Ni-DNA with full cyclic sweeps (-9 V→9 V→-9 V). The inset shows the current difference at zero voltage ($\Delta I_{V=0}$).

Figure 3 (a) Input voltage across Ni-DNA. The blue, black, and red lines are positive writing, no writing, and negative writing. (b) The corresponding currents flow through Ni-DNA. The red and blue curves are the responses after performing negative writing and positive writing for 50 sec. The black curves are the result of no writing. The upper and lower curves of the same colorized curves are positive and negative reading, respectively.

Figure 4 EIS profiles of Bax Ni-DNA and p53-Bax complex. The black, red and blue spots denoted the bare gold, the Ni-DNA with Bax promoter and the p53-Bax complex, respectively.

Figure 1.

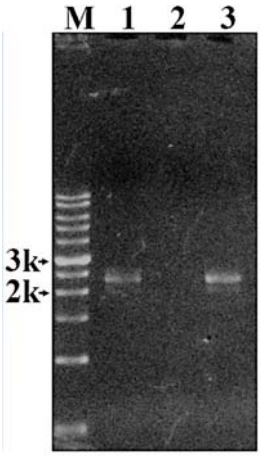

Figure 2.

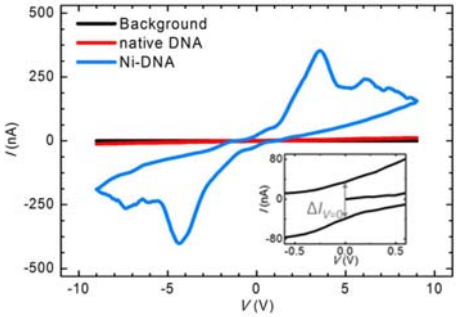

Figure 3.

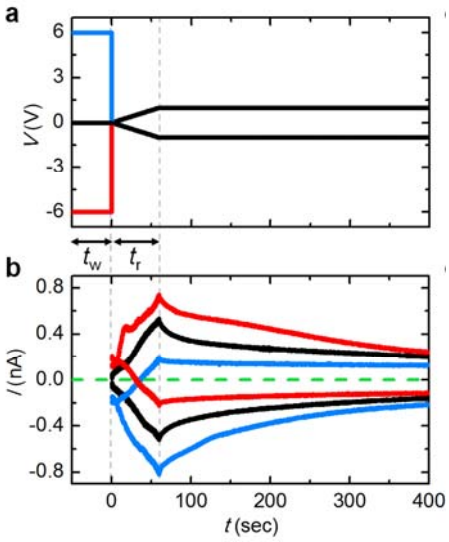

Figure 4.